Conserved epitope on influenza-virus hemagglutinin head defined by a vaccine-induced antibody

Donald D. Raymond[a,1,2], Goran Bajic[a,1], Jack Ferdman[b], Pirada Suphaphiphat[b], Ethan C. Settembre[b], M. Anthony Moody[c,d], Aaron G. Schmidt[a], and Stephen C. Harrison[a,e,3]

[a]Laboratory of Molecular Medicine, Boston Children's Hospital, Harvard Medical School, Boston, MA 02115; [b]Seqirus, Cambridge, MA 02139; [c]Department of Pediatrics, Duke University Medical School, Durham, NC 27710; [d]Duke Human Vaccine Institute, Duke University Medical School, Durham, NC 27710; and [e]Howard Hughes Medical Institute, Boston, MA 02115

Contributed by Stephen C. Harrison, November 22, 2017 (sent for review September 5, 2017; reviewed by Steven Gamblin and Scott E. Hensley)

Circulating influenza viruses evade neutralization in their human hosts by acquiring escape mutations at epitopes of prevalent antibodies. A goal for next-generation influenza vaccines is to reduce escape likelihood by selectively eliciting antibodies recognizing conserved surfaces on the viral hemagglutinin (HA). The receptor-binding site (RBS) on the HA "head" and a region near the fusion peptide on the HA "stem" are two such sites. We describe here a human antibody clonal lineage, designated CL6649, members of which bind a third conserved site ("lateral patch") on the side of the H1-subtype, HA head. A crystal structure of HA with bound Fab6649 shows the conserved antibody footprint. The site was invariant in isolates from 1977 (seasonal) to 2012 (pdm2009); antibodies in CL6649 recognize HAs from the entire period. In 2013, human H1 viruses acquired mutations in this epitope that were retained in subsequent seasons, prompting modification of the H1 vaccine component in 2017. The mutations inhibit Fab6649 binding. We infer from the rapid spread of these mutations in circulating H1 influenza viruses that the previously subdominant, conserved lateral patch had become immunodominant for individuals with B-cell memory imprinted by earlier H1 exposure. We suggest that introduction of the pdm2009 H1 virus, to which most of the broadly prevalent, neutralizing antibodies did not bind, conferred a selective advantage in the immune systems of infected hosts to recall of memory B cells that recognized the lateral patch, the principal exposed epitope that did not change when pdm2009 displaced previous seasonal H1 viruses.

influenza vaccine | hemagglutinin | B-cell memory | affinity maturation

Influenza viruses reinfect previously immune hosts by acquiring escape mutations in the epitopes of neutralizing antibodies (1). Thus, a central question for next-generation influenza vaccines is how to focus the immune response on epitopes with restricted variability (2, 3). Attention has concentrated largely on two conserved regions on the influenza virus hemagglutinin (HA), the so-called "stem" and the receptor binding site (RBS) on the HA "head."

The HA sequences of H1N1 viruses from 1977 to 2009 vary most at positions of residues on the outward-facing surface of the head, the surface most exposed on virions and thus the region of the molecule most accessible to antibodies (Fig. 1). The conserved RBS, at the center of this surface, is a known target of broadly neutralizing antibodies (4). Because the site is smaller than a typical antibody footprint, however, surrounding variable residues often limit the breadth of any particular RBS-directed response. Certain antibodies with long complementarity-determining region (CDR) H3 loops can contact the conserved residues while avoiding many of the variable positions around the RBS perimeter (4, 5), and two or three distinct antibodies of this kind may share contacts with only the conserved positions, requiring multiple HA mutations to escape neutralization by an immune response that includes all of them (4).

Unlike the HA head, the stem has been largely invariant. Although some of the conservation may be due to functional constraints, as this part of the molecule has two very different conformational states (prefusion and postfusion), variation at many positions in the stem is possible without compromising viral replicative fitness (6). Because the surface of the stem is occluded on virions, it has been under little, if any, evolutionary pressure from human B-cell immunity during the past 100 y (1). Protection by stem antibodies in animal models appears to come from Fc effector functions, rather than from infectivity neutralization (i.e., from recognition of HA on the cell surface just before budding, not from HA on the mature virion) (7, 8). Were stem-directed immunity widespread in the human population, variation and subsequent viral resistance within this region could emerge, as suggested by recent studies in which virus was passaged in the continuous presence of anti-stem antibodies or donor immune sera (9).

Herd immunity drives antigenic drift of seasonal influenza viruses. Even when they reduce or eliminate neutralization, however, the accumulating mutations in HA do not completely prevent binding to previously elicited antibodies, and thus exposure to drifted virus still allows recall of memory B cells (10,

Significance

Antigenic variation requires frequent revision of annual influenza vaccines. Next-generation vaccine design strategies aim to elicit a broader immunity by directing the human immune response toward conserved sites on the principal viral surface protein, the hemagglutinin (HA). We describe a group of antibodies that recognize a hitherto unappreciated, conserved site on the HA of H1 subtype influenza viruses. Mutations in that site, which required a change in the H1 component of the 2017 vaccine, had not previously "taken over" among circulating H1 viruses. Our results encourage vaccine design strategies that resurface a protein to focus the immune response on a specific region.

Author contributions: D.D.R., G.B., M.A.M., A.G.S., and S.C.H. designed research; D.D.R., G.B., J.F., and M.A.M. performed research; P.S., E.C.S., and S.C.H. supervised research; D.D.R., G.B., J.F., P.S., E.C.S., M.A.M., A.G.S., and S.C.H. analyzed data; and D.D.R., G.B., A.G.S., and S.C.H. wrote the paper.

Reviewers: S.G., The Francis Crick Institute; and S.E.H., University of Pennsylvania.

Conflict of interest statement: J.F., P.S., and E.C.S. are employees of Seqirus, which has research and development programs related to influenza vaccines. The other authors declare no conflict of interest.

Data deposition: The sequences reported in this paper have been deposited in the GenBank database (accession nos. MF458174 and MF458175). The atomic coordinates and structure factors have been deposited in the Protein Data Bank, www.wwpdb.org (PDB ID codes 5W6C and 5W6G).

[1]D.D.R. and G.B. contributed equally to this work.

[2]Present address: Broad Institute, Cambridge, MA 02142.

[3]To whom correspondence should be addressed. Email: harrison@crystal.harvard.edu.

This article contains supporting information online at www.pnas.org/lookup/suppl/doi:10.1073/pnas.1715471115/-/DCSupplemental.

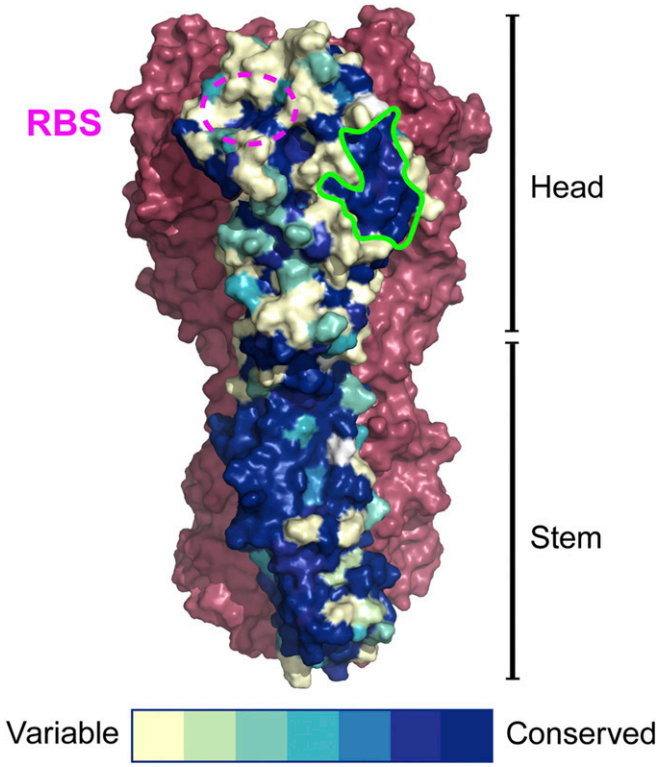

Fig. 1. Conservation of surface residues in H1 HAs (1977–2009). Conservation is shown on the surface of an HA monomer on a scale from beige (most variable) to dark blue (most conserved). The RBS and the conserved lateral patch are outlined in pink and green, respectively.

11). Subsequent affinity maturation by selection of somatic mutations "updates" that memory, generating new pressure on HA and starting a new cycle in an evolutionary "arms race" (10, 12). The introduction in 2009 of an H1N1 virus (pdm2009) quite distant from those circulating from 1977 to 2008 changed the antigenic landscape abruptly, rather than gradually. Exposure to the pdm2009 virus could have elicited recall only for antibodies recognizing epitopes, such as those on the stem, present on prepandemic H1N1 viruses and conserved across the 2009 shift. Indeed, following exposure to pdm2009, either by infection or vaccination, subjects in several studies showed a strong response to stem epitopes, but those responses did not persist after subsequent vaccination (13). A similar transience of the stem response in the general population would have reduced any sustained selection for escape, and indeed, no fixed changes in the stem have occurred. Instead, a K166Q mutation that appeared during the 2013–2014 flu season is now present in 99% of all H1N1 isolates (14). Fixation of this mutation, together with appearance of an adjacent N-linked glycosylation site (at position 165) in somewhat more recent strains (e.g., A/Michigan/45/2015, A/Singapore/GP1908/2015), determined the first revised H1N1 vaccine strain recommendation since 2009.

Residues 165 and 166 lie in a surface patch on the side of the HA head that was nearly invariant in human H1 isolates between 1977 and 2012 (Fig. 1). It has no known functional significance. Conservation of this "lateral patch" suggests that there was little selective pressure on the composition of the epitopic surface, and that cognate antibodies may have been rare during most of the 32 y between 1977 and 2009. The 2009 antigenic shift appears to have focused a much larger component of the antibody response on the lateral patch epitope, one of the few sites at which cognate memory B cells were already present. Prevalence of such antibodies would then have selected for fixation of the K166Q mutation (14).

We describe here an antibody clonal lineage, members of which recognize the lateral patch (Fig. 2*A*). We suggest that this lineage, CL6649 (named after one of its members), represents the type of response that ultimately selected for the K166Q mutation. CL6649 derives from subject 7 in a clinical trial of an adjuvanted, monovalent, A/California/07/2009 X-181 (pdm2009) vaccine (15). The subject, born in 1975, had not been exposed to the 2009 pandemic strain at the time of vaccination. Antibodies from this lineage bind H1 HAs from 1977 to 2009 and hence representatives of two distinct H1 pandemics (Fig. 3). Their footprint includes residues 165 and 166. The properties of CL6649 are consistent with the inferences described above concerning the K166Q mutation (14, 16). Introduction of the pdm2009 virus, to which most of the generally prevalent antibodies did not bind, would have favored recall of those rare memory B cells with BCRs that recognized the lateral patch, transforming a previously subdominant response into a dominant one.

Results

Ab6649 Binds HAs Spanning 30 y of Antigenic Drift. Antibodies in the lineage with the greatest representation among sequences from Siena subject 7 B cells, CL6515, bind the RBS; they depend on a mutation in the vaccine strain likely to have been due to egg adaptation (17). The second largest lineage from this donor included 19 paired-chain sequences (Fig. 2*A*). Initial analysis showed that one of its members, Ab6649, neutralized A/California/07/2009, a pdm2009 viral isolate, and A/Solomon Islands/03/2006 (Fig. 2*B*). Selected members of the CL6649 antibody lineage did not compete, or competed only marginally, with Ab6639 from CL6515 (Fig. 2*C* and Fig. S1). We analyzed the CL6649 phylogeny and inferred the unmutated common ancestor (UCA) and its intermediates (Fig. 2*A*). We determined the affinity of the UCA and of Ab6649 for a panel of HAs from influenza strains representing 30 y of antigenic drift and two pandemics (Fig. 3). All measurements used antigen-binding fragments (Fabs) and HA1 "head" domains, to avoid complications from multivalency. The UCA bound the HA head of A/USSR/92/1977, but had no detectable affinity for any other HA tested (Fig. 3). These data suggest that exposure to an H1N1 strain circulating 2–3 y after the subject's birth in 1975 may have elicited the UCA. Fab6649 bound HA from strains isolated from 1977 to 2009, including pdm2009 and its vaccine strain, X-181; thus, its breadth of binding included HAs from two distinct H1N1 pandemics. Neither the UCA nor 6649 bound HAs from H3, H5, H7, or B influenza viruses (Fig. 3).

Structure of Fab6649 Bound with HA from A/Solomon Islands/03/2006. We determined the crystal structure of Fab6649 bound with trimeric HA from A/Solomon Islands/03/2006 (Fig. 4*A* and Table S1). The Fab engages an epitope on the side of the HA1 head domain. It approaches HA with its long axis normal to the trimer threefold axis (Fig. 4*A*) and contacts the head with both heavy and the light chains. CDRs L1 and L3 bind a conserved loop (residues 125–128; H3 numbering, used here throughout), while CDRH3 and framework residues of the heavy chain contact the edge of β5, the strand farthest from the trimer threefold axis. The antigen-combining site includes 12 hydrogen bonds, six with main-chain carbonyls or amides on HA (Fig. 4*B*). Sequences of HAs from H1N1 influenza viruses circulating from 1977 to 2009 and mapped onto the HA structure show that the Fab6649 epitope was conserved during that entire period (Fig. 1). Conservation of the Ab footprint and dominance of main-chain interactions at the antigen–antibody interface likely account for the observed breadth.

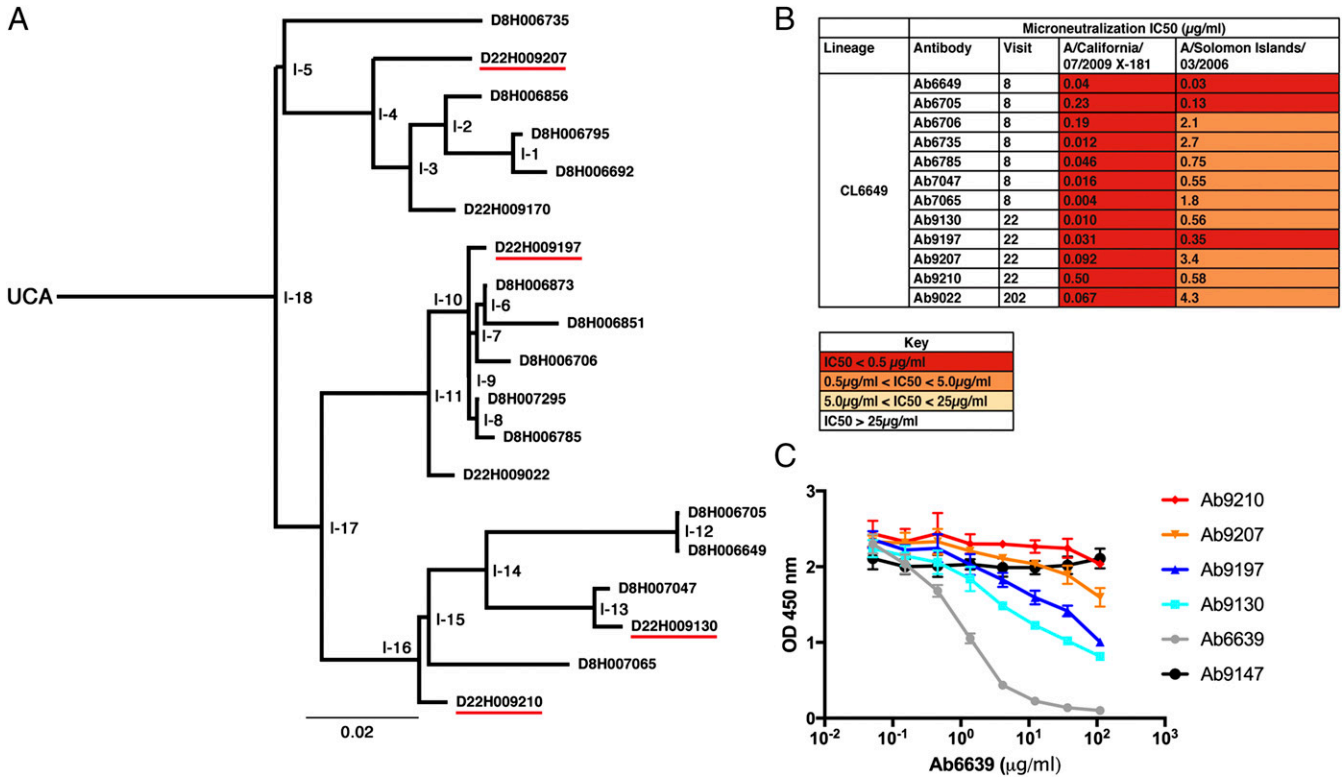

Fig. 2. (*A*) Phylogenetic analysis of the CL6649 clonal antibody lineage. Antibody lineage members that were characterized further are underscored in red. (*B*) Neutralization of selected H1 influenza viruses by antibodies from the CL6649 clonal lineage. Neutralization titers (50%) for the indicated influenza viruses and mAbs are shown. All neutralization assays were carried out with a minimum of three replicates. Color-coding indicates arbitrary neutralization potency. (*C*) Direct competition ELISA of selected CL6649 lineage members, underlined in *A*, with a previously characterized RBS-binding Ab6639 (17). An unrelated antibody, Ab9147, served as a control.

Structure of CL6649 UCA, the Rearranged Germ Line Precursor. We determined the crystal structure of the UCA to gain information about affinity maturation in this lineage. The structure showed that CDR loop conformations in the antigen-combining site had remained essentially invariant between the UCA and Ab6649 (Fig. 4*C*). During the course of affinity maturation, however, four tyrosine residues in the UCA (Y33 and Y93 in the light chain and Y35 and Y54 in the heavy chain) had mutated to phenylalanines (Fig. 4*C*), making the binding interface more hydrophobic. Light chain Y93 does not contact the antigen; the other three all have nonpolar contacts, but only light chain Y33 may have lost a hydrogen bond when losing the phenolic hydroxyl. The increased hydrophobicity of the antibody–antigen interface and the reduced requirement for hydrogen-bond complementarity appear to have contributed to the increased breadth acquired during affinity maturation.

Viral Escape. A mutation (K166Q) in the HA of new pdm2009-like H1N1 viruses (14) has been suggested as the cause of reduced vaccine efficacy for the 2013–2014 season and onward. Recent viral isolates (e.g., A/Singapore/GP1908/2015 and A/Michigan/45/2015; Global Initiative on Sharing All Influenza Data accession nos. EPI862697 and EPI830246, respectively) also include an N-linked glycosylation site at residue 165. The most recent World Health Organization vaccine recommendations include an H1N1 strain with both changes. Residues 165 and 166 are within the Fab6649 footprint. We determined whether they influence Fab6649 affinity by measuring binding with single S165N and K166Q and double S165N/K166Q pdm2009 HA head mutants (Fig. 5 *A* and *B*). The substitution K166Q substantially reduced Fab6649 affinity. The S165N mutation had no effect, but the absence of any shift in SDS/PAGE mobility suggests lack of glycosylation at the 165–167 NKS motif in the recombinant HA head (Fig. 5*C*). The double mutation, S165N/K166Q, which did show a mobility shift, nearly abolished Fab6649 binding; the two mutations appeared to have additive effects. We infer, in accordance with earlier suggestions (14, 16), that recall from memory of antibodies with footprints overlapping that of Ab6649 is likely to have selected for the altered epitope in circulating pdm2009-like viruses.

Discussion

The inferred UCAs of both CL6515 and CL6649 bind the HA of H1 A/USSR/92/1977, an H1N1 isolated 2 y after the birth date of Siena subject 7, suggesting that the lineages originated in response to a 1977-like influenza infection during the donor's childhood. The CL6649 UCA bound only the 1977 HA (of those we tested), but Ab6649 and several others from the lineage bound H1 HAs spanning more than 30 y of antigenic variation, indicating that somatic mutation had continually updated the specificity as the donor responded to subsequent exposures (from infection or vaccination). Receipt of the pdm2009 vaccine then focused the response on the most conserved sites exposed on the virion: the RBS and the lateral patch. Strong selection between 2009 and 2015 for the mutations at positions 165 and 166 indicates the development of widespread herd immunity directed at this epitope (14, 16), and thus the sequence of immune response events we have inferred for Siena subject 7 may represent that of many individuals of similar age. The lateral patch site is sufficiently large to allow antibodies with various CDR structures to bind, however, and we cannot yet judge from this single example the extent to which Ab6649 represents a

Subtype	HA strain	HA binding K_D (μM)	
		UCA	Fab6649
H1	A/USSR/90/1977	30.57	1.12
	A/Maryland/12/1991	>100	0.94
	A/Solomon Islands/03/2006	>100	2.12
	A/California/07/2009	>100	0.64
H3	A/Victoria/3/1975	>100	>100
	A/Philippines/2/1982	>100	>100
	A/Johannesburg/33/1994	>100	>100
	A/Victoria/361/2011	>100	>100
H5	A/Vietnam/1203/2004	-	>100
	A/gyrfalcon/ Washington/41088-6/2014	-	>100
H7	A/Shanghai/2/2013	-	>100
Vic	B/Malaysia/2506/2004	-	>100
Yama	B/Florida/04/2006	-	>100
	B/Phuket/3073/2013	-	>100

Key
K_D < 1 μM
1 μM < K_D < 10 μM
10 μM < K_D < 50 μM
K_D > 50 μM

Fig. 3. Affinity measurements of Fab6649 and UCA. Fab fragments of 6649 and UCA were screened for binding with heads of seasonal H1, H3, H5, H7, and B influenza HAs that circulated during the donor's lifetime. Color-coding indicates the apparent K_d, measured by BLI.

prevalent clonotype or a "typical" binding mode for the antibodies in many individuals that evidently selected for the mutations now present in most of the circulating H1N1 viruses.

Explanations for conservation of the lateral patch might be some as-yet unexplained compromise in viral fitness from changes in that region or partial occlusion by adjacent HAs tightly packed on the virion surface. Careful inspection of images from electron cryotomography suggests that the latter explanation is unlikely. Moreover, H3 viruses circulating since 1968 have a similar conserved patch on the lateral surface of the HA head, but in that case, immune escape probably appeared early, through the introduction of N-glycans at positions 165 and 245, around 1968 and 1986, respectively (Influenza Research Database; https://www.fludb.org/brc/home.spg?decorator=influenza). Thus, the lateral patch is apparently both antigenic on virions and immunogenic in infected individuals.

We have no direct evidence bearing on the possible loss of fitness of H1 viruses bearing HAs mutated at the Ab6649 site. We note that approximately 15 y after the 1918 pandemic, mutations appeared at positions 165 and 166, which reverted within a decade (Influenza Research Database; https://www.fludb.org/brc/home.spg?decorator=influenza). As these were some of the earliest mutations to be retained consistently for even a 3-y period, reversion might imply either a lack of widely distributed immune pressure or a minor disadvantage of the mutations for assembly, stability, or infectivity of the virus particle (or both).

Previous analyses of the antibody response to a first administration of a pdm2009 vaccine also found a prevalence of antibodies sensitive to changes at position 166, but without further structural information (16, 18, 19). Lineages encoded by gene segments V_H3~7 and J_H6 were especially prominent. In one study, of 157 clones analyzed by sorting and sequencing plasmablasts obtained at 7 d after vaccination, 138 (88%) were sensitive to mutation of residue K166 (K163 in the numbering used in that paper) (16). In that individual, approximately one-half of the clones (including one very large lineage) came from recombination events involving V_H3~7*01 and J_H6*02, with a CDRH3 of 18 residues. The extent of somatic hypermutation indicated that most or all of the clones were recall responses, just as we have inferred for clonal lineages CL6515 and CL6649. Another study found a similar convergence, with overrepresentation of V_H3~7 and J_H6 (18). The V_H3~7 antibodies may have had HA contacts distinct from those of the V_H4~39- and J_H5-encoded CL6649 antibodies, although they evidently overlapped in the vicinity of residue 166. Moreover, not all antibodies sensitive to the residue at 166 restrict their contacts to the conserved, lateral patch; for example, antibody 2D1 (20) covers position 166, but

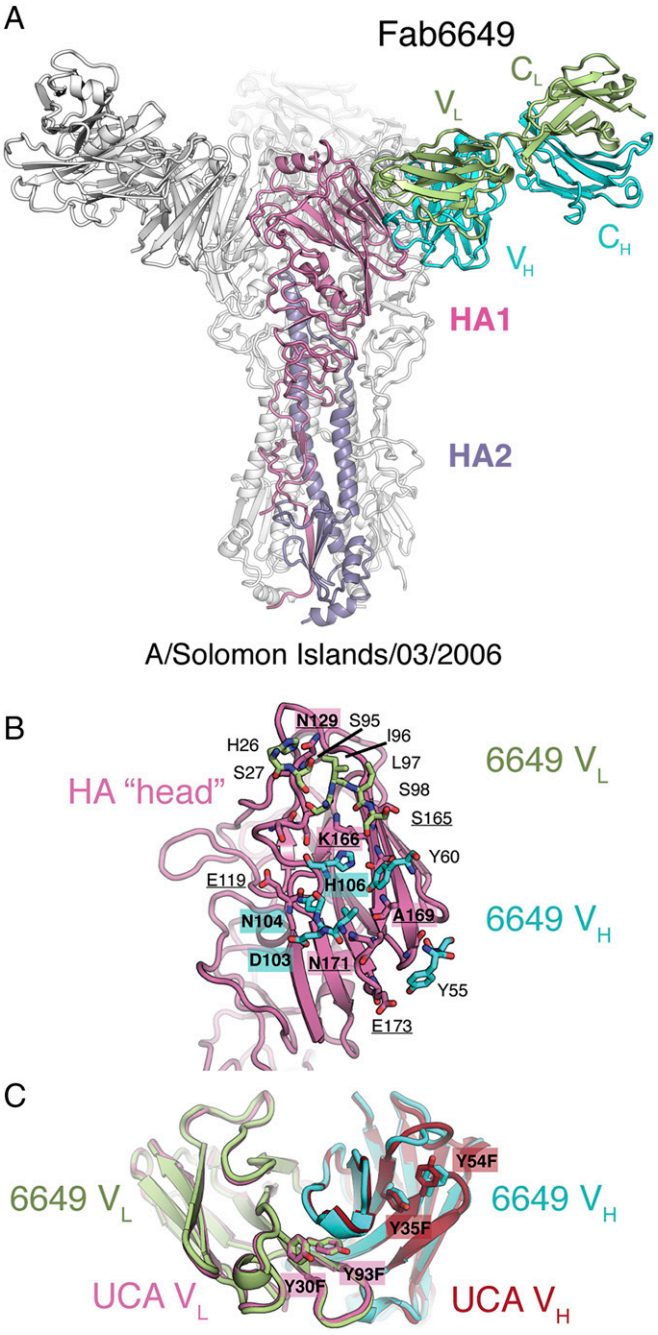

Fig. 4. Structures of Fab6649 bound with an HA and of the unbound UCA of the lineage. (*A*) Overall structure of Fab6649 bound with A/Solomon Islands/03/2006. HA1 and HA2 are colored pink and purple, respectively. Fab6649 contacts the HA1 head with both its heavy (teal) and light (green) chains. (*B*) Blow-up of the Fab:HA complex. Interface residues are shown as sticks and their positions indicated; those on HA are underscored. (*C*) Structures of the UCA and Fab6649 superposed. The comparison shows no structural rearrangements. Four tyrosine residues in the UCA that mutated during the course of affinity maturation to phenylalanines in Fab6649 are labeled.

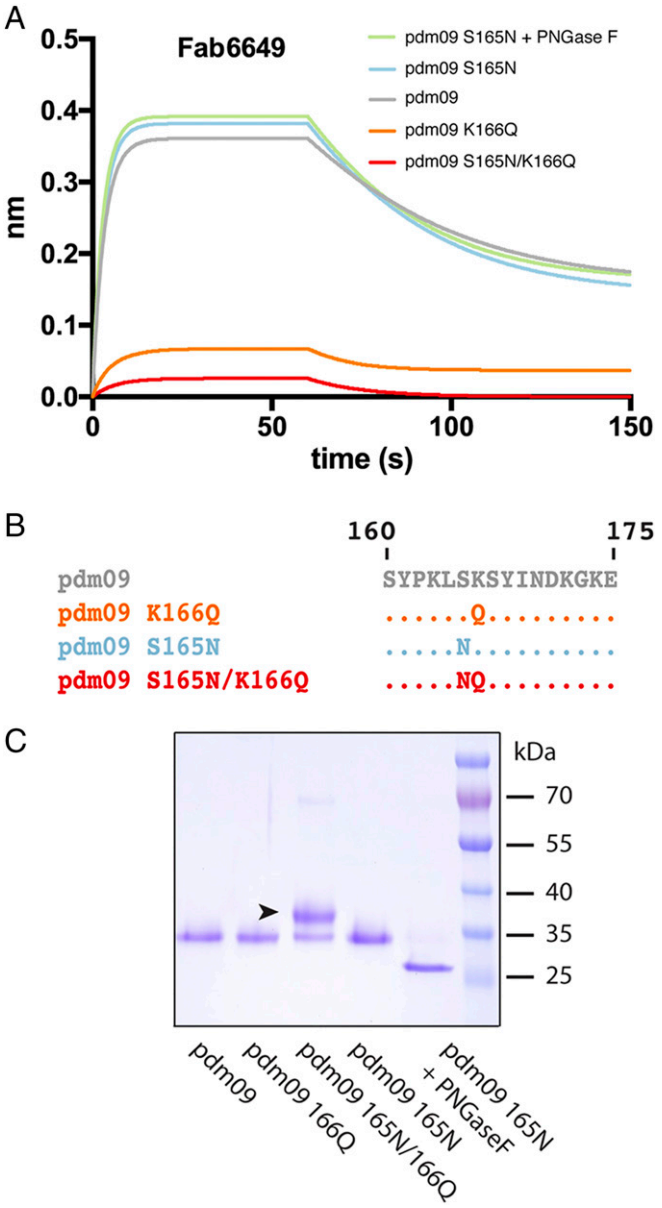

Fig. 5. In vitro characterization of HAs of the newly emerged pdm2009-like H1N1 viral isolates. (*A*) BLI measurements. Representative Langmuir fits of the binding isotherms generated by BLI with immobilized Fab6649 and the indicated pdm2009 HA head variants as "single hit" analytes at 5 μM. (*B*) Amino acid sequence alignment of pdm2009-like HAs. Dots indicate identities. Color-coding is as in *A*. (*C*) SDS/PAGE of HEK293F cell produced HA head variants. The arrow indicates the lower mobility band at 37 kDa of the S165N/K166Q variant, indicating N165 glycosylation on most of the HA polypeptide chains.

also engages the variable 156 loop on HA and sites at 129 and 131 that sometimes bear glycans. Ab6649 is insensitive to glycosylation at the latter two positions.

The foregoing studies provide further examples of a focused response due to selective conservation of a restricted region across an antigenic shift. Earlier work on responses to pdm2009 had also pointed to that mechanism in both infection and vaccination, mainly for stem-directed antibodies in the former case and for unidentified head epitopes in the latter (11, 21). Because the focusing will have depended on recall, however, the exposure histories of the different cohorts, and of the different individuals within them, may have influenced which epitopes dominated.

Conversion of a subdominant epitope into a dominant one is a goal of various proposed vaccine strategies for both HIV-1 and for influenza virus (22). The data presented here and the historical record of circulating variants suggest that the history of the H1N1 virus is an example—by natural infection, rather than vaccination—of just this process. The abrupt change (antigenic shift) in 2009 was in effect a resurfacing of the H1N1 HA, leaving one exposed epitopic region (the lateral patch) unchanged and another (the RBS) with surrounding residues in common with some previous seasonal HAs. The equally conserved stem, which on virions is nearly inaccessible to a B-cell receptor, was probably a less effective immunogenic surface during infection, although stem antibodies did appear to dominate early responses to pdm2009 infection in some individuals (11). The emergence of resistance to antibodies such as Ab6649, after many decades of conservation, suggests that widespread immunization with stem-exposed proteins might similarly select for resistance mutations not previously fixed. Vaccines designed to elicit polyclonal responses targeting more than one conserved epitope might avoid such an outcome.

Materials and Methods

Clonal Lineage Determination and Inference. We used the program Cloanalyst (23, 24) to annotate isolated paired heavy-light VDJ/VJ sequences, to infer intermediates and the UCA, and to reconstruct the phylogenetic tree of the clonal lineage.

Cloning, Expression, and Purification. We obtained monoclonal antibodies from a participant (Siena pt 7) in the clinical trial (at Novartis Vaccines) of an experimental H1 A/California/04/2009 (pdm2009) vaccine (15). Plasmacytes were sorted from an individual who was administered an experimental vaccine (developed by Novartis) for pandemic 2009 H1N1. Blood was drawn before vaccination and at days 8, 22 and 202 after vaccination, followed immediately by isolation and cryopreservation of peripheral blood mononuclear cells.

The study was conducted in accordance with the Declaration of Helsinki. The protocol and all documents related to the study were reviewed and approved by the Ethics Committee of the Azienda Ospedaliera Universitaria Senese. A complete description of procedures and the statement of Ethics Committee approval and informed consent are available elsewhere (15). Subsequent steps were carried out at the Duke Human Vaccine Institute, following published protocols (25). Paired-chain sequencing of the rearranged Ig heavy and light chain genes from single plasmablasts yielded influenza-specific antibodies, many of which belonged to distinct clonal lineages. Genes encoding the variable domains of Ab6649 and its UCA were synthesized and cloned for mammalian cell expression using a tissue plasminogen activation signal sequence. A 6xHis tag (noncleavable or cleavable) was added to the C terminus of the heavy-chain first constant domain. Fabs were produced by transient transfection, with PEI, of 293T cells adapted for suspension. Supernatants were harvested at 6 d after transfection and clarified by centrifugation. Fabs were purified using Co-NTA (Clontech) agarose, followed by gel filtration chromatography on a Superdex 200 column (GE Healthcare) in 10 mM Tris·HCl pH 7.5 and 150 mM NaCl. Purified Fabs were concentrated to >15 mg/mL and stored at 4 °C.

Codon-optimized cDNA of the recombinant ectodomain of H1 A/Solomon Islands/03/2006 HA (rHA) containing a C-terminal foldon trimerization and a 6xHis tag was subcloned into a pFastBac vector. *Trichoplusia ni* (Hi5) cells were infected with the recombinant baculovirus, and at 72 h postinfection, the supernatant was harvested and clarified by centrifugation. The rHA was purified using Co-NTA metal affinity resin. The bound protein was washed with 20 column volumes of PBS (10 mM sodium phosphate and 137 mM NaCl, pH 7.4) before elution with 500 mM imidazole. The eluted protein was dialyzed against PBS and incubated overnight with PreScission protease (Thermo Fisher Scientific) at a 1:100 molar mass ratio to remove the foldon and 6xHis purification tags. rHA was further purified by orthogonal Co-NTA agarose chromatography, followed by gel filtration chromatography in 10 mM Tris·HCl pH 7.5 and 150 mM NaCl. rHA was not activated by the addition of trypsin, and the resulting protein was uncleaved HA0. The purified protein was concentrated to >10 mg/mL and stored at 4 °C. Production and purification of HA1 head constructs were performed as described previously (4).

Microneutralization. Madin–Darby canine kidney cells were cultured in suspension in a proprietary medium (Seqirus) with shaking at 37 °C. Before the

assay, cells were pelleted and resuspended in DMEM (12-604F; Lonza) with 10% FBS and penicillin-streptomycin (17-602E; Lonza). A half-area microtiter plate (3696; Corning) was seeded with 2×10^4 cells and incubated for 6 h at 37 °C. Antibodies were normalized to a concentration of 100 μg/mL in DPBS (17-512F; Lonza). Fourfold serial dilutions of the antibodies were performed in DMEM with 1% BSA (BSA-30) and penicillin-streptomycin starting at a concentration of 25 μg/mL. Antibody dilutions were incubated with virus for 2 h at 37 °C and then added to cells after the medium was replaced with DMEM with 10% FBS and penicillin-streptomycin. After overnight incubation at 37 °C, the supernatant was aspirated, and the cells were fixed with a 1:1 mixture of acetone and methanol for 1 h at −20 °C. Plates were washed with DPBS with 0.05% Tween-20, blocked with DPBS with 2% BSA, and stained using anti-influenza A nucleoprotein (MAB8251; EMD Millipore), followed by Alexa Fluor 488-conjugated goat anti-mouse IgG (H+L) Ab (A11001; Invitrogen). Stained foci were counted with an ImmunoSpot Analyzer (Cellular Technology Limited). Results were summarized as the ratio (×100) of infected cells present in a given sample to the average in the control wells without antibody for that plate (% infectivity). Fig. 2*B* reports the concentration of antibody at which the percentage of infectivity fell to 50. All neutralization assays were carried out with a minimum of three replicates.

Crystallization and Structure Determination. Fab6649 was incubated with H1 A/Solomon Islands/03/2006 HA ectodomain at a 1.3:1 molar ratio. Complexes were separated from excess Fab6649 by gel filtration on a Superdex 200 column in 10 mM Tris·HCl pH 7.5 and 150 mM NaCl, and concentrated to 13 mg/mL Crystals were grown for 3 d at 20 °C by hanging-drop vapor diffusion from a 1:1 mixture of reservoir solution containing 1.9 M ammonium sulfate and 0.1 M Hepes, pH 7. Crystals of the UCA Fab grew in 26% PEG 2K MME, 0.15 M ammonium sulfate, and 0.1 M sodium acetate, pH 4.6. The crystals were cryoprotected by soaking in reservoir solution with 25% (for complex) or 10% glycerol (for UCA Fab), harvested into loops, and flash-cooled by plunging into liquid N_2.

Diffraction data were collected at 100 K on the NE-CAT 24 ID-C beamline at the Advanced Photon Source, Argonne National Laboratory. Diffraction images were indexed, integrated, and scaled using XDS (26). A subunit of A/Solomon Islands/03/2006 HA trimer (Protein Data Bank ID code 5UGY) and a homologous Fab (Protein Data Bank ID code 3H42) served as search models for molecular replacement with Phaser (27). Density modification was performed with DM (28), and model rebuilding was done with Coot (29). Refinement was performed with BUSTER (Global Phasing) or Phenix (30, 31). Figures were prepared with the PyMOL Molecular Graphics System v 1.8.6.0 (Schrödinger). The H3 numbering scheme was used for HA.

Bio-Layer Interferometry and Affinity Analysis. Bio-layer interferometry (BLI) experiments were performed using the BLItz system (Pall Fortébio). Fab was immobilized on a Ni-NTA biosensor, and the cleaved HA globular head was allowed to bind until saturation. For pdm2009 mutants, the inverse setup was used; the 6xHis-tagged rHA head was immobilized, and tag-cleaved Fabs were allowed to bind until saturation. Equilibrium dissociation constants (K_d) were obtained in GraphPad Prism version 6.0d by fitting saturation data from eight independent runs at different HA concentrations, using nonlinear least squares regression: $\mathrm{BLI} = B_{max} \times [\mathrm{HA}]/(K_d + [\mathrm{HA}])$, where B_{max} is the BLI signal at maximal binding and [HA] is the concentration of HA ectodomain.

Peptide-N-Glycosidase F Treatment. Enzymatic removal of N-linked glycans was performed with PNGase F (P0704; New England BioLabs) under native conditions. In brief, 100 μg of mammalian cell-produced HA heads at 1.25 mg/mL were incubated with 500 units of PNGase F overnight at 37 °C in 10 mM Tris·HCl and 150 mM NaCl. Deglycosylation was verified on a Coomassie blue-stained SDS/PAGE gel.

ACKNOWLEDGMENTS. We thank Giuseppe Del Giudice, Oretta Finco, Philip Dormitzer, and Shaun Stewart for their participation in earlier stages of this project; Thomas Kepler for assistance with Clonalyst; and Barton Haynes for advice and support. The research was supported by National Institutes of Health (NIH) Grant P01 AI089618. X-ray diffraction data were collected on Northeastern Collaborative Access Team beamline 24 ID-C (Advanced Photon Source), funded by NIH Grant P41 GM103403. The Pilatus 6M detector on 24-ID-C is funded by an NIH Office of Research Infrastructure Programs High-End Instrumentation Grant (S10 RR029205). This research used resources of the Advanced Photon Source, a US Department of Energy (DOE) Office of Science User Facility operated for the DOE Office of Science by Argonne National Laboratory under Contract DE-AC02-06CH11357. S.C.H. is an Investigator at the Howard Hughes Medical Institute.

1. Knossow M, Skehel JJ (2006) Variation and infectivity neutralization in influenza. *Immunology* 119:1–7.
2. Krammer F, Palese P (2015) Advances in the development of influenza virus vaccines. *Nat Rev Drug Discov* 14:167–182.
3. Victora GD, Wilson PC (2015) Germinal center selection and the antibody response to influenza. *Cell* 163:545–548.
4. Schmidt AG, et al. (2015) Viral receptor-binding site antibodies with diverse germline origins. *Cell* 161:1026–1034.
5. Whittle JR, et al. (2011) Broadly neutralizing human antibody that recognizes the receptor-binding pocket of influenza virus hemagglutinin. *Proc Natl Acad Sci USA* 108:14216–14221.
6. Doud MB, Bloom JD (2016) Accurate measurement of the effects of all amino acid mutations on influenza hemagglutinin. *Viruses* 8:E155.
7. DiLillo DJ, Palese P, Wilson PC, Ravetch JV (2016) Broadly neutralizing anti-influenza antibodies require Fc receptor engagement for in vivo protection. *J Clin Invest* 126: 605–610.
8. DiLillo DJ, Tan GS, Palese P, Ravetch JV (2014) Broadly neutralizing hemagglutinin stalk-specific antibodies require FcγR interactions for protection against influenza virus in vivo. *Nat Med* 20:143–151.
9. Anderson CS, et al. (2017) Natural and directed antigenic drift of the H1 influenza virus hemagglutinin stalk domain. *Sci Rep* 7:14614.
10. Fonville JM, et al. (2014) Antibody landscapes after influenza virus infection or vaccination. *Science* 346:996–1000.
11. Wrammert J, et al. (2011) Broadly cross-reactive antibodies dominate the human B cell response against 2009 pandemic H1N1 influenza virus infection. *J Exp Med* 208: 181–193.
12. Schmidt AG, et al. (2015) Immunogenic stimulus for germline precursors of antibodies that engage the influenza hemagglutinin receptor-binding site. *Cell Rep* 13:2842–2850.
13. Andrews SF, et al. (2015) Immune history profoundly affects broadly protective B cell responses to influenza. *Sci Transl Med* 7:316ra192.
14. Linderman SL, et al. (2014) Potential antigenic explanation for atypical H1N1 infections among middle-aged adults during the 2013-2014 influenza season. *Proc Natl Acad Sci USA* 111:15798–15803.
15. Faenzi E, et al. (2012) One dose of an MF59-adjuvanted pandemic A/H1N1 vaccine recruits pre-existing immune memory and induces the rapid rise of neutralizing antibodies. *Vaccine* 30:4086–4094.
16. Huang KY, et al. (2015) Focused antibody response to influenza linked to antigenic drift. *J Clin Invest* 125:2631–2645.
17. Raymond DD, et al. (2016) Influenza immunization elicits antibodies specific for an egg-adapted vaccine strain. *Nat Med* 22:1465–1469.
18. Jackson KJ, et al. (2014) Human responses to influenza vaccination show seroconversion signatures and convergent antibody rearrangements. *Cell Host Microbe* 16: 105–114.
19. Krause JC, et al. (2011) Epitope-specific human influenza antibody repertoires diversify by B cell intraclonal sequence divergence and interclonal convergence. *J Immunol* 187:3704–3711.
20. Xu R, et al. (2010) Structural basis of preexisting immunity to the 2009 H1N1 pandemic influenza virus. *Science* 328:357–360.
21. Li GM, et al. (2012) Pandemic H1N1 influenza vaccine induces a recall response in humans that favors broadly cross-reactive memory B cells. *Proc Natl Acad Sci USA* 109: 9047–9052.
22. Haynes BF, Kelsoe G, Harrison SC, Kepler TB (2012) B-cell-lineage immunogen design in vaccine development with HIV-1 as a case study. *Nat Biotechnol* 30:423–433.
23. Kepler TB (2013) Reconstructing a B-cell clonal lineage, I: Statistical inference of unobserved ancestors. *F1000 Res* 2:103.
24. Kepler TB, et al. (2014) Reconstructing a B-cell clonal lineage, II: Mutation, selection, and affinity maturation. *Front Immunol* 5:170.
25. Moody MA, et al. (2011) H3N2 influenza infection elicits more cross-reactive and less clonally expanded anti-hemagglutinin antibodies than influenza vaccination. *PLoS One* 6:e25797.
26. Kabsch W (2010) XDS. *Acta Crystallogr D Biol Crystallogr* 66:125–132.
27. McCoy AJ, et al. (2007) Phaser crystallographic software. *J Appl Crystallogr* 40: 658–674.
28. Cowtan K, Main P (1998) Miscellaneous algorithms for density modification. *Acta Crystallogr D Biol Crystallogr* 54:487–493.
29. Emsley P, Cowtan K (2004) Coot: Model-building tools for molecular graphics. *Acta Crystallogr D Biol Crystallogr* 60:2126–2132.
30. Adams PD, et al. (2011) The Phenix software for automated determination of macromolecular structures. *Methods* 55:94–106.
31. Afonine PV, et al. (2012) Towards automated crystallographic structure refinement with phenix.refine. *Acta Crystallogr D Biol Crystallogr* 68:352–367.